

Award Number: MIPR 1GCDGB1102

TITLE: Evaluation of Chronic Stress Induced Neurodegeneration
and Treatment Using an *In Vivo* Retinal Model

PRINCIPAL INVESTIGATOR: Heike Rentmeister-Bryant, Ph.D.
Randolph Glickman, Ph.D.
Andy Tsin, Ph.D.
Rowe Elliott

CONTRACTING ORGANIZATION: Naval Health Research Center Detachment
Brooks Air Force Base, Texas 78235-5665

REPORT DATE: May 2003

TYPE OF REPORT: Annual

PREPARED FOR: U.S. Army Medical Research and Materiel Command
Fort Detrick, Maryland 21702-5012

DISTRIBUTION STATEMENT: Approved for Public Release;
Distribution Unlimited

The views, opinions and/or findings contained in this report are those of the author(s) and should not be construed as an official Department of the Army position, policy or decision unless so designated by other documentation.

20040121 057

REPORT DOCUMENTATION PAGEForm Approved
OMB No. 074-0188

Public reporting burden for this collection of information is estimated to average 1 hour per response, including the time for reviewing instructions, searching existing data sources, gathering and maintaining the data needed, and completing and reviewing this collection of information. Send comments regarding this burden estimate or any other aspect of this collection of information, including suggestions for reducing this burden to Washington Headquarters Services, Directorate for Information Operations and Reports, 1215 Jefferson Davis Highway, Suite 1204, Arlington, VA 22202-4302, and to the Office of Management and Budget, Paperwork Reduction Project (0704-0188), Washington, DC 20503

| | | | | |
|--|---|--|--|----------------------------------|
| 1. AGENCY USE ONLY (Leave blank) | | 2. REPORT DATE May 2003 | 3. REPORT TYPE AND DATES COVERED Annual (1 May 2002 - 30 Apr 2003) | |
| 4. TITLE AND SUBTITLE Evaluation of Chronic Stress Induced Neurodegeneration and Treatment Using an In Vivo Retinal Model | | | 5. FUNDING NUMBERS MIPR 1GCDGB1102 | |
| 6. AUTHOR(S) Heike Rentmeister-Bryant, Ph.D. Randolph Glickman, Ph.D. Andy Tsin, Ph.D. Rowe Elliott | | | | |
| 7. PERFORMING ORGANIZATION NAME(S) AND ADDRESS(ES) Naval Health Research Center Detachment Brooks Air Force Base, Texas 78235-5665 E-Mail: Heike.Rentmeister-Bryant@navy.brooks.af.mil | | | 8. PERFORMING ORGANIZATION REPORT NUMBER | |
| 9. SPONSORING / MONITORING AGENCY NAME(S) AND ADDRESS(ES) U.S. Army Medical Research and Materiel Command Fort Detrick, Maryland 21702-5012 | | | 10. SPONSORING / MONITORING AGENCY REPORT NUMBER | |
| 11. SUPPLEMENTARY NOTES Original contains color plates. All DTIC reproductions will be in black and white. | | | | |
| 12a. DISTRIBUTION / AVAILABILITY STATEMENT Approved for Public Release; Distribution Unlimited | | | | 12b. DISTRIBUTION CODE |
| 13. ABSTRACT (Maximum 200 Words) This project is developing the snake eye/Scanning Laser Ophthalmoscope model for use as a longitudinal damage model in the study of neural injury/neurodegenerative disease. This model is an in vivo, non-invasive imaging technique and provides the unique ability to observe cellular changes in the retina. Progress has been made in three areas of research necessary to establish the snake eye as a model for human neural injury/disease: (1) Morphology: a) A pilot study on determining the effects of treating retinal laser injury with near infrared light did not show promise for saving damaged photoreceptors. b) Photochemical lesions are more difficult to produce, and are almost undetectable after only one week. (2) Electrophysiology: A technique to record pattern electroretinographic responses from the snake eye has been developed, and will be used for visual function testing; and (3) Biochemistry: the study of the cellular make up of the rat snake retina is ongoing, and is providing further evidence that this retina is an all cone retina. | | | | |
| 14. SUBJECT TERMS Neurodegeneration, Retinal injury, Retinal function, Snake eye, Laser, Photoreceptor, confocal Scanning Laser Ophthalmoscope | | | | 15. NUMBER OF PAGES 17 |
| | | | | 16. PRICE CODE |
| 17. SECURITY CLASSIFICATION OF REPORT Unclassified | 18. SECURITY CLASSIFICATION OF THIS PAGE Unclassified | 19. SECURITY CLASSIFICATION OF ABSTRACT Unclassified | 20. LIMITATION OF ABSTRACT Unlimited | |

NSN 7540-01-280-5500

Standard Form 298 (Rev. 2-89)
Prescribed by ANSI Std. Z39-18
298-102

Table of Contents

| | |
|-----------------------------------|----|
| Cover..... | 1 |
| SF 298..... | 2 |
| Table of Contents..... | 3 |
| Introduction..... | 4 |
| Body..... | 6 |
| Key Research Accomplishments..... | 13 |
| Reportable Outcomes..... | 14 |
| Conclusions..... | 15 |
| References..... | 16 |
| Appendices..... | |

INTRODUCTION

The objective of this project is to develop an *in vivo* model for the study of retinal injury following thermal and/or photochemical laser injuries. This model may also be applicable as a damage model for the investigation of a number of neurodegenerative disorders, such as Parkinson's disease. Previous studies with this *in vivo* snake eye model (Elliott et al., 1998; Zwick et al., 2000) have shown promise for the study of the mechanisms underlying retinal injury, repair and treatment. The further development of the confocal Scanning Laser Ophthalmoscope (cSLO) / snake eye model will require a basic examination of the visual system of these animals to understand the differences and similarities to other vertebrate eyes, as they pertain to retinal injury. Thus as we examine retinal injury in the snake eye we are also collecting background data on the snake's visual system.

The unique optical properties of the snake's eye permit the imaging of retinal structures in cellular detail through the natural pupil (Figure 1), and subjects require only light anesthesia, even for longitudinal studies of retinal changes following laser exposure (Figures 2 and 3). These SLO images are equivalent in some ways, to histological samples from the eyes of other retinal injury models (commonly used are monkey, rabbit, rat, and mouse models).

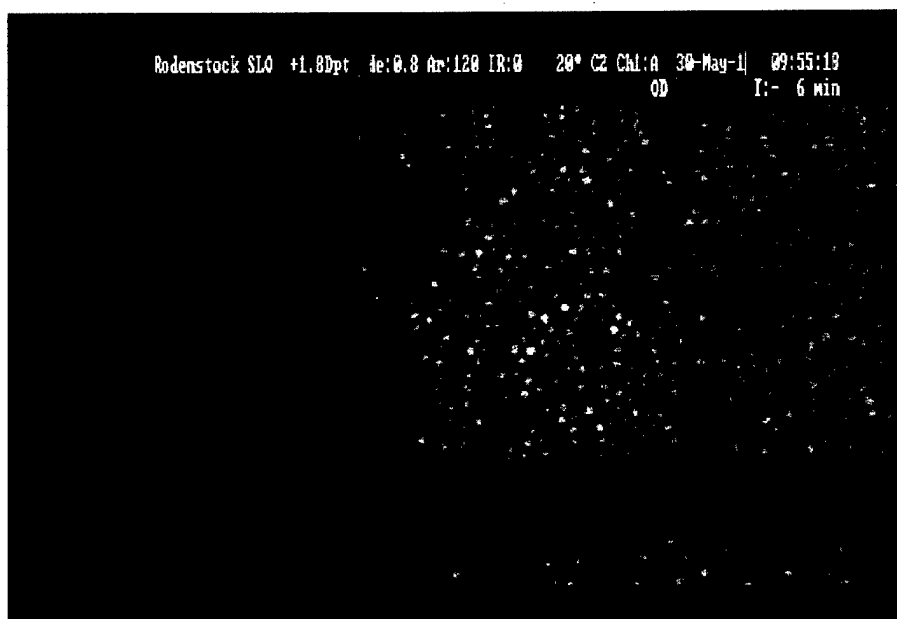


Figure 1: Photoreceptor matrix of an intact *in vivo* rat snake eye, imaged with a cSLO. This is an all cone retina, similar in this respect, to the human macula. Cell spacing is $\sim 10\text{-}12\ \mu$.

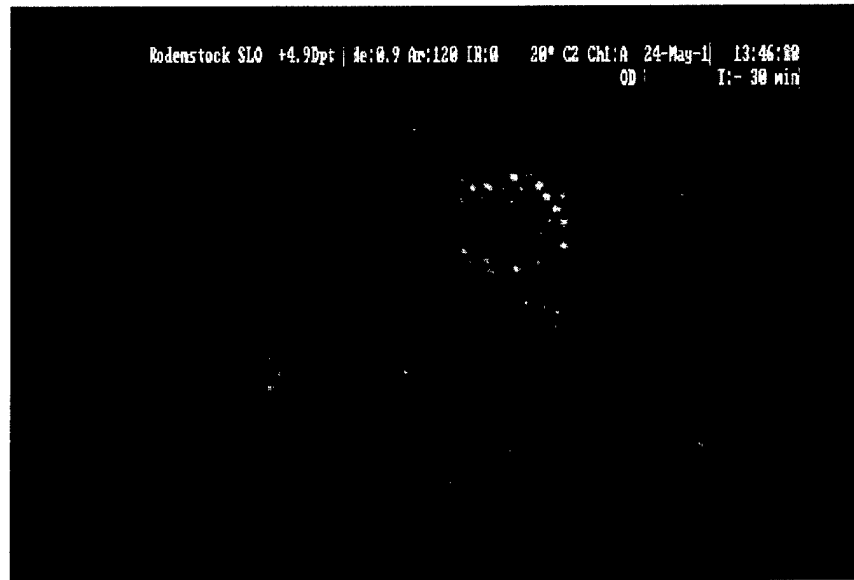


Figure 2: Thermal retinal injury at 1-hr post-exposure. A core of destroyed cells is surrounded by a number of damaged and distinct, yet still structurally intact photoreceptors. These are the cells that are the target of a potential treatment.

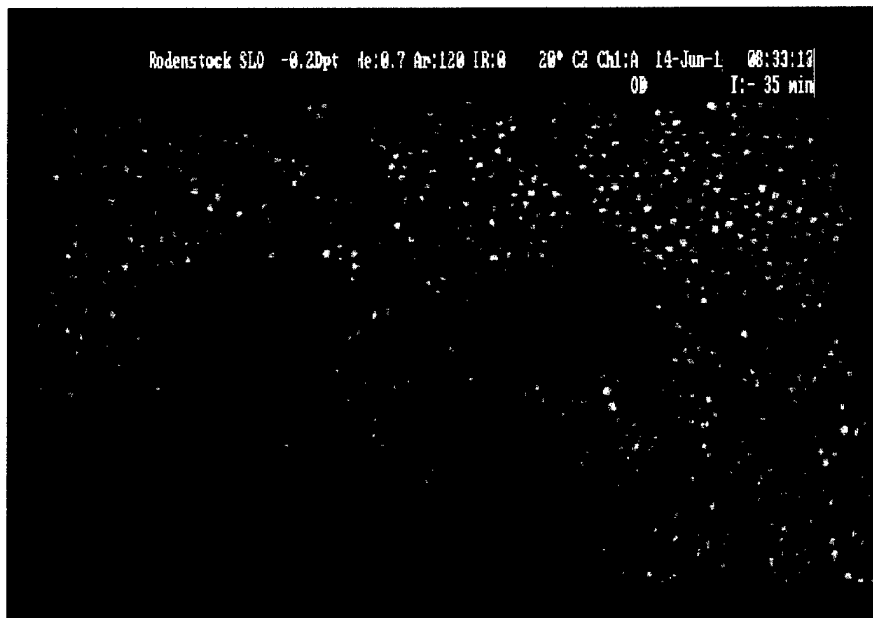


Figure 3: Same lesions at 3-wks post-exposure. The damaged cells are now missing and the size of the lesion has increased considerably.

BODY

Our work with this damage model follows three general areas:

1. Morphological examination of retinal injury and treatment;
2. Electrophysiology and visual function (baseline and post retinal injury); and
3. Examination of visual pigments and detailed histological examination of retinal structures to verify SLO derived images.

1. Morphological studies:

Over the past twelve months, we have continued pilot experimentation with fluorescent imaging of the dyes, 2',7'-dichlorodihydrofluorescein diacetate (Molecular Probes, D-399) and 5-(and-6)-carboxy-2',7'-dichlorodihydrofluorescein diacetate (C-400). These photochemical markers are specific for reactive oxygen species in the cell. Dye was injected IC into anesthetized subjects at 30-minutes post exposure. Retinal imaging was done using the cSLO's internal fluorescein filters at various light levels and imaging parameters. These experiments validated and further elucidated the contribution of oxidative stress to laser-induced retinal injury.

We have completed pilot experimentation on a proposed approach using near infrared light as a treatment for laser retinal injury. The SLO has an internal laser for retinal illumination at the 760 nm wavelength. This laser is designed for ICG dye excitation, among other things, and is thus capable of operation at power levels above that necessary to produce a putative beneficial effect (Eells et al., 2003), albeit at a suboptimal wavelength. Alternatively the LED source for red light used in Eells' study could be used. The 760 nm laser is capable of 2 mW output, allowing for an energy density at the retina of approximately 0.6 W/cm^2 . The cSLO's scan area, at the 20-degree field setting, illuminates a rectangle of retina in the snake eye of approximately 450×750 micrometers in linear dimensions. Two subjects received four thermal laser lesions with an individual spot size of $\sim 100 \mu\text{m}$ in a randomly chosen eye. Lesions were placed such that, post lesion, the retinal space containing two adjacent lesions could receive infrared laser treatment, while leaving the other two lesions as untreated controls (Diagram 1).

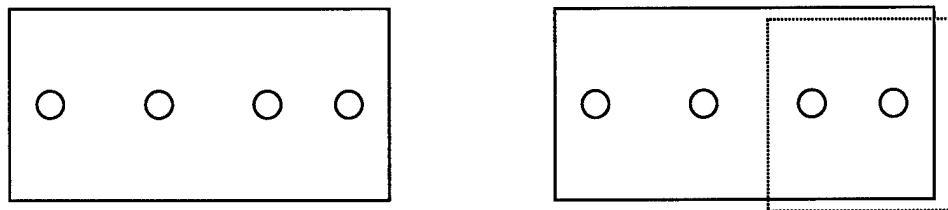


Diagram 1. Left: Linear array of laser lesions, each spot size approximately $100 \mu\text{m}$ diameter with $300 \mu\text{m}$ spacing between lesions. Right: Representative illustration of 760 nm laser treatment area for two lesions in a four lesion set. This precision in tissue area treated, allows side-by-side comparison of treated and untreated lesions.

Treatments were repeated across three days. Morphological changes were tracked across several days using the imaging capabilities of the cSLO. Based solely on visual inspection of the images, we were unable to determine a beneficial effect of infrared light on laser-induced retinal injuries.

Using a solid state 473 nm laser as the exposure source we began investigation of the photochemical laser injury in the snake eye. Exposures were made in three different subjects in an attempt to bracket the optimal exposure parameters. In the final session in this series, photochemical lesions were observed at 2.5mW x 40-second laser exposure. These lesions appeared only 24 hours post exposure and resolved completely after two weeks. The lesions were faint, best imaged w/ infrared illumination and appeared to be anterior (that is more in the inner retina) than thermal lesions. After this session, the 473nm source laser malfunctioned, and was returned to the manufacturer for warranty repair.

2. Electrophysiological studies:

In addition to its imaging capabilities, the cSLO can also be modulated externally to produce stimulus patterns directly on the subject's retina for psychophysical or electrophysiological testing. In the present module of the NETP project, we have demonstrated that a pattern electroretinogram (PERG) can be recorded from the snake's eye by direct stimulation of the retina with counterphased square wave gratings produced by the cSLO. The advantage of this method is that the region of retina under investigation may be imaged and stimulated simultaneously in order to evaluate visual function. In the next phase of the study, the PERG will be used as an objective measure of visual function in the retina following laser injury.

Three Great Plains rat snakes (*Elaphe guttata emoryi*) were studied. Animals were anesthetized with an intramuscular injection of ketamine/zylazine in a ratio of 3.5:1, respectively; at an approximate dose of the combined drugs of 75 mg/kg. A Rodenstock cSLO was used to image the snake retina. Animals were placed in a custom-made holder that allowed their eyes to be positioned at the aperture of the cSLO.

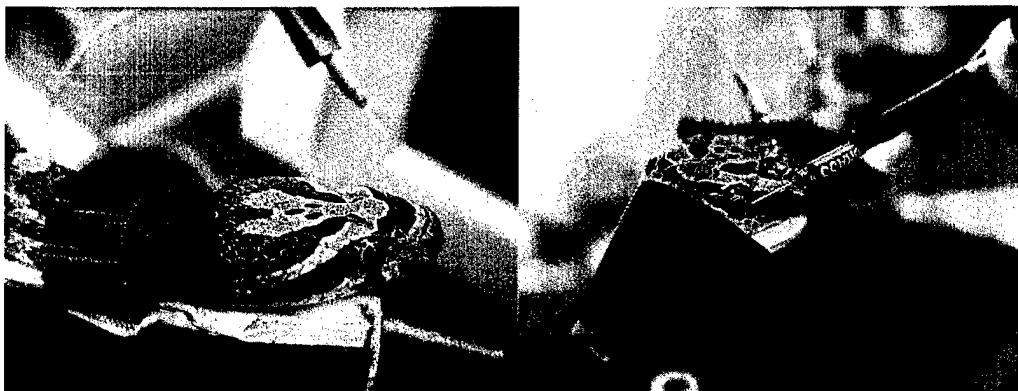


Figure 4: Left: Rat snake shown anesthetized and placed in custom-made holder
Right: Needle electrode positioned for recordings of ERGs and PERGs.

PERG responses were elicited with high contrast, counterphased square wave gratings projected on to the snake's retina. The stimulus gratings were generated by a computer-based visual stimulator (VisionProbe®, San Antonio, TX). The VisionProbe controlled the acousto-optical modulator of the cSLO, which in turn drove the cSLO's HeNe laser (632.8 nm) to produce the grating stimuli on the animal's retina. During visual stimulation, the retina was simultaneously imaged with the cSLO to ensure that the eye was stable during the electrophysiological recording period. A clear, specialized scale called the spectacle, which is electrically nonconductive, covers the snake's eye. In order to record the PERG, a small incision was made in the spectacle near the limbus, without injuring the cornea. The tip of a Grass needle electrode was placed into the incision. Electrical contact was improved by occasionally applying a drop of Ringer's on the electrode tip-tissue junction.

Electrophysiological responses were amplified using a Grass Neurodata 12 amplifier with frequency bandpass limits set from 1 to 1 KHz. Amplified signals were acquired with the Experimenter's Workbench® system (DataWave, Longmont, CO). Two methods of signal processing were used. For conventional signal averaging, the PERG's were acquired for 30 sec and averaged at the temporal frequency of the counterphased gratings. Alternatively, a lock-in amplifier referenced to the stimulus grating counterphase rate was used for real-time retrieval of the responses (Glickman et al., 1991). A block diagram of the experimental setup is shown in Figure 5.

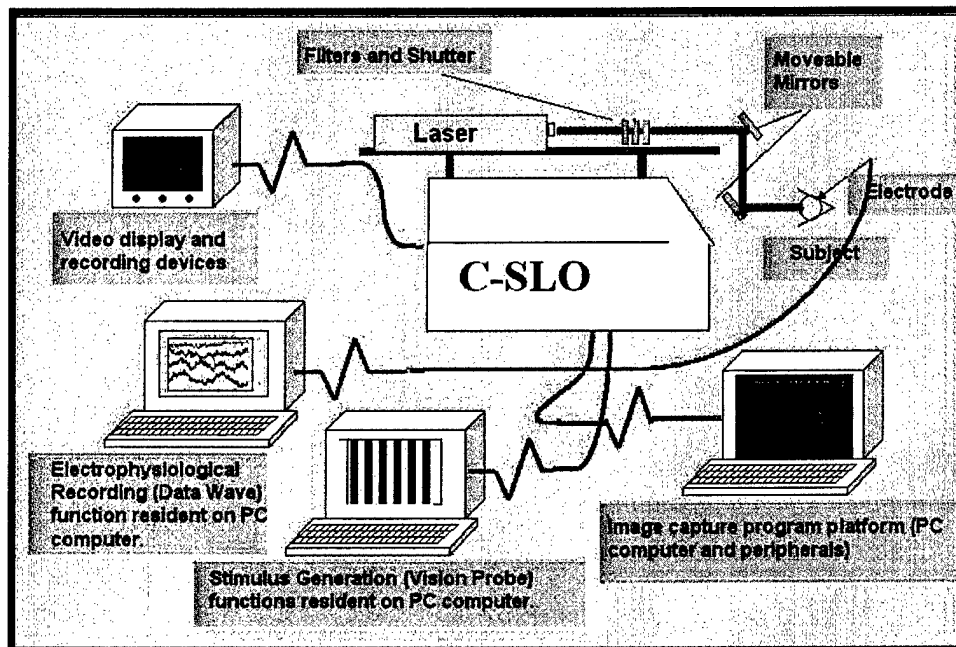


Figure 5: Block diagram of cSLO-based, PERG recording system.

In order to demonstrate the integrity of the electrophysiological recording system, a conventional flash ERG was elicited from the snake's eye. A Grass photostimulator was set to an intermediate intensity and triggered by the data acquisition computer. The ERG responses to twenty flashes were acquired and averaged. A conventional ERG waveform was obtained, exhibiting the standard ERG response components, i.e., a-, b-, and c-waves, as shown in Figure 6.

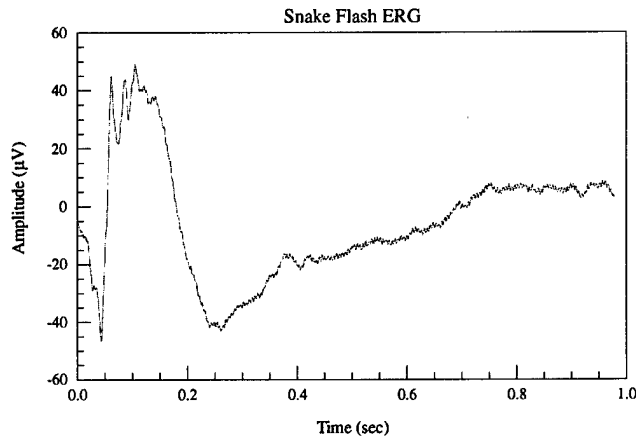


Figure 6: Flash ERG elicited from the rat snake; waveform in figure is the average of 20 individual flashes. The a-wave occurred at an implicit time of 40 msec, the b-wave peak at about 120 msec, and the onset of the c-wave is apparent by about 275 msec. Oscillatory potentials are present on the rising phase of the b-wave.

The pattern ERG response is formally elicited by retinal stimuli producing changing contrast, but no net change in luminance. These stimulus conditions were met by generating counterphasing, high-contrast, square wave gratings with the cSLO, and projecting these grating patterns directly onto the snake's retina. The PERG response consisted of an electrical potential generated across the eye by each reversal of the square wave grating. The spatial frequency (i.e. the number of light/dark bars per degree of visual angle) and temporal frequency (the number of complete cycles of pattern reversals per second; for example, a 1 Hz grating undergoes two pattern reversals per second) were varied in order to characterize the PERG. A set of PERG responses is shown in Figure 7. In terms of the optimal stimulus conditions, the maximum amplitude PERG was produced by square wave gratings with a 2 Hz temporal frequency, and 0.5-1.0 cycles per degree (cpd) spatial frequency.

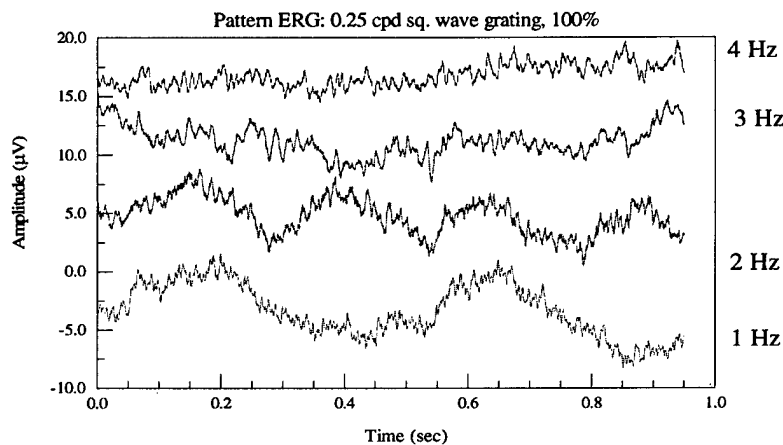


Figure 7: Pattern ERG elicited by counterphased square wave gratings. The stimulus condition consisted of a square wave grating at 0.25 cpd and 100% contrast, produced by the cSLO directly on the retina, and counterphased at the temporal frequencies indicated in the figure. The maximum PERG response was produced by a 2 Hz temporal frequency, and was unrecordable at 4 Hz.

In order to demonstrate that the PERG was evoked by a change of contrast (i.e. the stimulus pattern) and not by an overall luminance change, an experiment was done in which the grating pattern produced by the cSLO on the snake's retina was defocused by moving the confocal plane of the instrument away from the retinal photoreceptor layer. This caused a decrease in the stimulus contrast, and resulted in loss of the PERG amplitude and synchrony, proving that the recorded response was pattern-dependent. This experiment is illustrated in Figure 8.

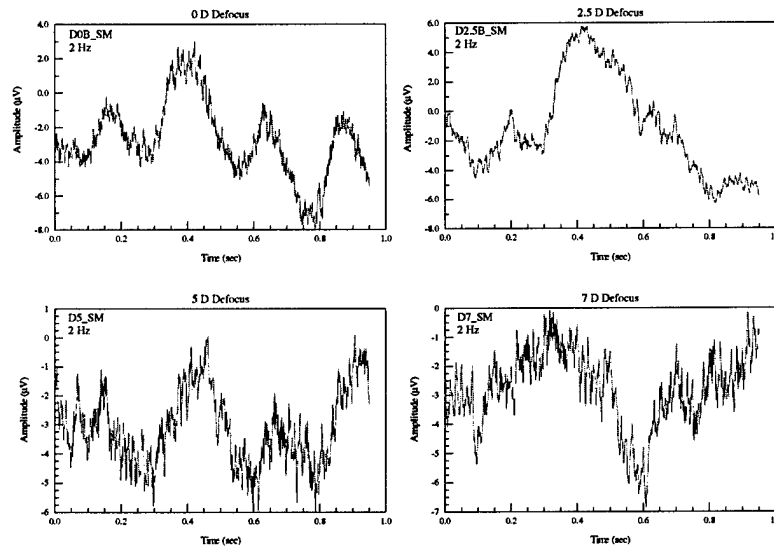


Figure 8. Amplitude of the PERG response was focus-dependent, proving that the response was pattern-evoked. The four panels in this figure show the resulting PERG recorded with progressive amounts of defocus. Top Left: 0 diopters (D) defocus (i.e. image is optimally focused on retina). Top Right: 2.5 D of defocus. Bottom Left: 5 D of defocus. Bottom Right: 7 D of defocus.

3. Visual Pigments and Histological analysis:

a) The biochemical analyses are still ongoing. Past studies have shown that retinyl esters in the eye are stored predominantly in retinal pigment epithelium (RPE). However, in cone-dominated species, such as chicken and ground squirrel, a higher ester concentration was found in retina rather than in RPE (Rodriguez & Tsin, 1989; Mata et al., 2002). Interestingly, we have found (Leal et al., 2002) a higher concentration of esters localized within rat snakes' RPE (0.3 - 0.6nmol/eye) versus their retina (.02-.05 nmol/eye).

Animals were light adapted and anesthetized before eye dissection. Retina and retinal pigment epithelium were isolated under a dissecting microscope, and retinoids were extracted with acetone. Separation of retinyl esters, retinal, and retinol was accomplished by using a five percent water deactivated alumina column before High Performance Liquid Chromatogram (HPLC) analyses. Retinoids were identified by retention time and online scan using a photodiode array detector. Quantitation was carried out by comparison with known amounts of authentic standards. Results are summarized below (Table 1).

Amount of Vitamin A in RPE and Retina measured by HPLC:

| Retina/RPE | Retina | | RPE | | Retinoid |
|--------------|-----------------------|----------------|-----------------------|---------------|-----------------|
| #Pooled | nmols/eye | | nmols/eye | | Total/eye |
| | 11cis-RP/AT-RP | | 11cis-RP/AT-RP | | |
| | | Total | | Total | |
| 2 | ND / .0346 | 0.0346 | ND / .137 | 0.137 | 0.1716 |
| 2 | ND / .02293 | 0.02293 | .01016 / .1055 | 0.1157 | 0.13859 |
| 2 | .0206 / .0279 | 0.0485 | .11 / .2085 | 0.3185 | 0.367 |
| 2 | .01 / .02 | 0.03 | .0119 / .0213 | 0.0332 | 0.0632 |
| 5 | .0428 / .112 | 0.1548 | .0137 / .0326 | 0.0463 | 0.2011 |
| 3 vs 2 | .0232 / .09385 | 0.11705 | .0073 / .0555 | 0.0628 | 0.179785 |
| 6 | Sample lost | | .019 / .493 | 0.512 | 0.512 |
| 6 | | | | | |
| (1/2 sample) | .0008 / .0045 | 0.0053 | .0337 / .216 | 0.2497 | 0.255 |
| (1/2 sample) | .002 / .0118 | 0.0138 | .043 / .306 | 0.349 | 0.3628 |
| 6 | ND / ND | ND | ND / .023 | 0.023 | 0.023 |
| 6 | ND / ND | ND | .02857 / .177 | 0.2056 | 0.20557 |
| | | | | | |
| | | | | | |
| | | | | | |
| | | | | | |

Table 1: Results of HPLC analyses. Note: 11cis-RP=11 *cis* retinyl palmitate; AT-RP= all-*trans* retinyl palmitate; 11 *cis*-AL= 11-*cis* retinal; AT-AL= all-*trans* retinal; AT-OL= all-*trans* retinol and ND= non detectable.

b) Histological Examinations: In addition to the biochemical analyses, we have conducted histological examinations to show that the photoreceptors of rat snakes have cone-like morphology. For this histological analysis, the rat snake's eyecups (upon removal) were immersed in fixative (2%-2% paraformaldehyde and glutaraldehyde in 0.081 mol phosphate buffer; pH 7.2), dehydrated with ethanol and embedded in Epon. Once embedded, an ultra-microtome was used to cut semi-thin sections of 1 μ m. After mounting, sections were stained with methylene blue and viewed under a light-microscope. The attached photomicrographs show that the rat snake has an all cone retina.

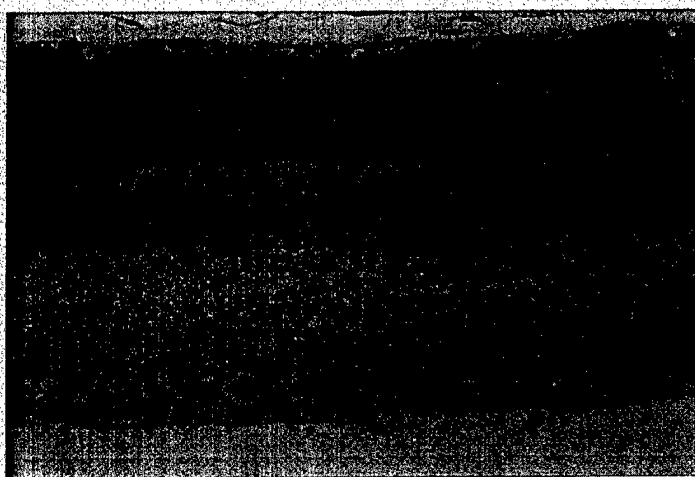
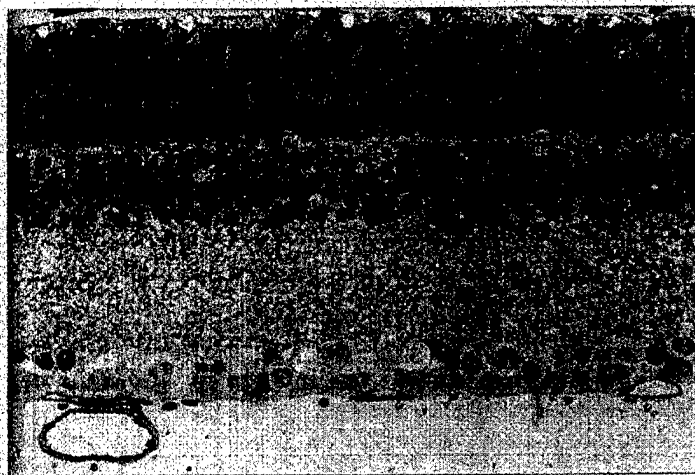


Figure 9: Cross section of the retina from the rat snake (*Elaphe g. guttata*), inner retina at the bottom, outer retina toward the top w/ photoreceptors (w/ adherent RPE pigment) in the uppermost strata.

c) Immunohistochemistry Studies: Presently, we are planning to label these photoreceptors with a cone-specific antibody to show that their photoreceptors are exclusively cone and not rod. To achieve this, we will use the cone-specific monoclonal antibody from COS-1 cells produced against photoreceptor membranes of the chicken. This antibody has been shown to label middle and long-wavelength-sensitive cones in tetrapods (Szel et al., 1986; Rohlich & Szel, 1993) as well as Large Single and Double cones of the garter snake [*Thamnophis sirtalis*]; Sillman et al., 1997]. We have already obtained this antibody from Dr. Rohlich (in Budapest) as well as antibodies for bovine rhodopsin (OS-2) from Dr. Hargrave (in Florida, for positive control) for this research. Tissue will be cryo-preserved and then sectioned before incubation with primary and then secondary antibody for visualization of the antigens.

KEY RESEARCH ACCOMPLISHMENTS

- Histochemical marker dyes, specific for reactive oxygen species in the cell, confirmed and elucidated the contribution of oxidative stress to laser-induced retinal injury.
- Near infrared light was tested as a potential treatment for laser retinal injury. We did not see any difference between treated and untreated lesions. However, infrared light administered at a different wavelength using a LED might differ in its beneficial effects from the cSLO's internal infrared laser.
- Pilot experimentation began in an attempt to determine the exposure parameters for producing photochemical lesions in the rat snake.
- A procedure was established using the cSLO to produce pattern stimuli directly on the snake's retina to elicit a pattern electroretinographic (PERG) response. The PERG will be used to evaluate visual function changes following laser injury.
- The retinoids identified in the ongoing biochemical analysis have been found to be atypical for a cone-dominated eye, but are consistent with crepuscular behavior and the scotopic vision of the rat snake.
- Histological examinations further demonstrate that the photoreceptors of rat snakes have cone-like morphology, and it is expected that labeling of these photoreceptors with cone specific antibody will show that they are exclusively cone and not rod.

REPORTABLE OUTCOMES

Presentations:

- Glickman, R.D., Elliott, W.R., Rentmeister-Bryant, H., & Tsin, A. (2002). Functional and cellular investigations of retinal laser bioeffects in a "small eye" model. Presented at the Ninth Annual Michaelson Research Conference, Portland, ME.
- Elliott, W.R., Glickman, R.D., Rentmeister-Bryant, H., & Zwick, H. (2003). Functional assessment of snake retina using pattern ERG. Invest. Ophthalmol. Vis. Sci. 44(5):E-2706; and (2003)
Presented at the 2nd Annual Retreat of the Center for Biomedical Neuroscience, UTHSCSA, San Antonio, TX.

Training supported by this award:

Robert Leal is a graduate student in the Biology MS (with thesis option) program at UTSA. He is currently performing the HPLC analyses of retinoids, and performed the histology work for this reporting period. He is supported by the NETP since spring 2002.

Funding applied for based on work supported by this award:

Project Title: "Using the snake model (*Elaphe g. emoryi*) for screening of potential treatment effects for retinal laser injuries using infrared radiation.

Funding Category applied for: DARPA "Persistence in combat" (6.1/6.2)

Funding result for FY04: The proposed statement of work for pilot experimentation was not funded.

CONCLUSIONS

The objective of this project is to develop an *in vivo* damage model for the study of the mechanisms underlying retinal injuries and other neurodegenerative disorders. For this purpose we have selected the snake eye with its unique suite of ocular properties, combined with the imaging capabilities of the confocal Scanning Laser Ophthalmoscope.

The cSLO/snake eye model has the advantage that we can observe same subject cellular level changes over time in an all cone photoreceptor retina. In order to establish this model for the study of neurodegeneration and human disease, we must continue to study the properties of the snake eye as well, and find the similarities and differences between snake and human vision.

Previous work characterized the spectral sensitivity of the flash ERG in the garter snake, which has an all-cone retina and is also a colubrid snake closely related to the rat snake (Jacobs et al., 1992), but to our knowledge this is the first report of a pattern-evoked electroretinographic response recorded from the rat snake's eye. It is also the first reported use of the cSLO for electrophysiological testing in a reptile model. Based on the observations reported here, the snake eye has relatively low acuity function, exhibiting a maximum PERG response with square wave gratings of less than 1 cpd or less, and at the relatively low temporal frequency of 2 Hz. Using the cSLO's ability to position stimuli at identified retinal loci, the PERG responses obtained did not reveal topographical specificity within the central 40 degrees of visual field.

The retinal responses recorded from the rat snake eye are more consistent with a rod-based retina, yet the morphology of the rat snake photoreceptors is more consistent with cone photoreceptors. Moreover, the previous work in this project on the biochemistry of the photoreceptors in the rat snake retina found a visual pigment profile similar to that of rod photoreceptors. The behavior of this animal is crepuscular (active at dawn and dusk), which also suggests that the rat snake's retinal photoreceptors are adapted to low-light conditions. We have hypothesized that the photoreceptors in the rat snake retina are cones, but have adapted to support mesopic vision. We are continuing to establish the baseline characteristics of the animal's visual response, in order to interpret the effects of the laser-induced retinal lesions that will be started in the next module of this project.

REFERENCES

- Eells, J.T., Henry, M.M., Summerfelt, P., Wong-Riley, M.T.T., Buchmann, E.V., Kane, M., Whelan, N.T., & Whelan, H.T. (2003). Therapeutic photobiomodulation for methanol-induced retinal toxicity. *Proceedings of the National Academy of Sciences of the United States of America*, 100(6):3439-3444.
- Elliott, R., Zwick, H., Wood, E., & Stuck, B. (1998). Utilization of acridine orange to characterize leucocyte activity in the snake retinal vascular system. *IOVS* 39(4):S-996.
- Glickman, R.D., Rhodes, J.W. & Coffey, D.J. (1991). Noninvasive techniques for assessing the effect of environmental stressors on visual function. *Neurosci. Biobehav. Rev.* 15, 173-178.
- Jacobs, G.H., Penwick, J.A., Crognale, M.A., & Deegan, J.F. II (1992). The all-cone retina of the garter snake: spectral mechanisms and photo pigment. *J. Comp. Physiol. A-Sens. Neural Behav. Physiol.* 170, 701-707.
- Leal, R., Tsin, A., Glickman, R., Elliott, R., & Rentmeister-Bryant, H. (2002). Ocular retinoids in corn snake (*Elaphe g. guttata*). *Invest. Ophthalmol. Vis. Sci.* 43 (ARVO Suppl.):144.
- Mata, N.L., Radu, R.A., Sclemmons, R., & Travis, G.H. (2002). Isomerization and Oxidation of Vitamin A in Cone-Dominant Retinas: A Novel Pathway for Visual Pigment Regeneration in Daylight. *Neuron*, 36, 1-20.
- Rodriguez, K.A., and Tsin, A.T. (1989). Retinyl esters in the vertebrate neuroretina. *American Journal of Physiology*, 256 (1 pt 2): p. R255-8.
- Rohlich P, and Szel A. (1993). Binding sites of photoreceptor-specific antibodies Cos-1, OS-2 and Ao. *Current Eye Research*, 12:935-944.
- Sillman, A.J., Govardovskii, V.I., Rohlich, P., Southard, J.A., & Loew, E.R. (1997). The photoreceptors and visual pigments of the garter snake (*Thamnophis sirtalis*): a microspectrophotometric, scanning electron microscopic and immunocytochemical study. *J Comp Physiol, A* 181: 89-101
- Szel, A., Takacs L., Monostori, E., Diamantstein, T., Vigh-Teichmann, I., & Rohlich, P. (1986). Monoclonal antibody-recognizing cone visual pigment. *Exp Eye Res* 43: 871-883.
- Zwick, H; Elliott, R; Li, G; Akers, A; Edsall, P; Stuck, ME (1999). In-vivo imaging of photoreceptor structure and laser injury pathophysiology in the snake eye. In: *Ophthalmic Technologies IX*, Rol, PO; Joos, KM; Manns, F; Stuck, BE; Belkin, M., Eds. *Proc. SPIE Vol. 3591*, 368-374.

Zwick, H., Elliott, R., & Edsall, P. (2000). A method for *in vivo* detection of photoreceptor oxidative stress induced by laser radiation. In: Protocols in Oxidative Stress, Ed. Don Armstrong. In press.